OPEN ACCESS Freely available online

PLOS ONE

IMACULAT — An Open Access Package for the Quantitative Analysis of Chromosome Localization in the Nucleus

Ishita Mehta[1☯], Sandeep Chakraborty[2*☯], Basuthkar J. Rao[3]

1 Department of Biological Sciences, Tata Institute of Fundamental Research, Mumbai, India, **2** Department of Biological Sciences, Tata Institute of Fundamental Research, Mumbai, India, **3** Department of Biological Sciences, Tata Institute of Fundamental Research, Mumbai, India

Abstract

The alteration in the location of the chromosomes within the nucleus upon action of internal or external stimuli has been implicated in altering genome function. The effect of stimuli at a whole genome level is studied by using two-dimensional fluorescence in situ hybridization (FISH) to delineate whole chromosome territories within a cell nucleus, followed by a quantitative analysis of the spatial distribution of the chromosome. However, to the best of our knowledge, open access software capable of quantifying spatial distribution of whole chromosomes within cell nucleus is not available. In the current work, we present a software package that computes localization of whole chromosomes - Image Analysis of Chromosomes for computing localization (IMACULAT). We partition the nucleus into concentric elliptical compartments of equal area and the variance in the quantity of any chromosome in these shells is used to determine its localization in the nucleus. The images are pre-processed to remove the smudges outside the cell boundary. Automation allows high throughput analysis for deriving statistics. Proliferating normal human dermal fibroblasts were subjected to standard a two-dimensional FISH to delineate territories for all human chromosomes. Approximately 100 images from each chromosome were analyzed using IMACULAT. The analysis corroborated that these chromosome territories have non-random gene density based organization within the interphase nuclei of human fibroblasts. The ImageMagick Perl API has been used for pre-processing the images. The source code is made available at www.sanchak.com/imaculat.html.

Citation: Mehta I, Chakraborty S, Rao BJ (2013) IMACULAT — An Open Access Package for the Quantitative Analysis of Chromosome Localization in the Nucleus. PLoS ONE 8(4): e61386. doi:10.1371/journal.pone.0061386

Editor: Ulrike Gertrud Munderloh, University of Minnesota, United States of America

Received November 12, 2012; **Accepted** March 7, 2013; **Published** April 8, 2013

Funding: This work was funded by the Tata Institute of Fundamental Research (Department of Atomic Energy). The funders had no role in study design, data collection and analysis, decision to publish, or preparation of the manuscript.

Competing Interests: The authors have declared that no competing interests exist.

* E-mail: sanchak@gmail.com

☯ These authors contributed equally to this work.

Introduction

DNA is folded and compacted in order to occupy the limited space within the cell nucleus wherein the genome replicates, transcribes and translates to form proteins [1]. Another important revelation in the field of genomics came from the finding that the genomes are positioned in a non-random manner in the cell nucleus [2–5]. The organized genome and the machineries required for its maintenance and function within the nucleus, along with other nuclear components make up the nuclear architecture [6–8]. The organization of the genome within the nucleus and its interaction with nuclear components alter during both development and in disease. This non-random chromosomal positioning within the architectural framework of the nucleus is thought to be a critical dimension of genome function [5,8–11].

Chromosome territories occupy a non-random and a radial distribution within interphase nuclei [2–5,10,12,13]. Although genomic entities are arranged in this patterned organization, they are not rigid compartments but instead are dynamic structures that can be repositioned with respect to other nuclear structures and other genomic regions [14]. In addition, dynamic repositioning of whole chromosome territories has also been observed during differentiation [8,15–19] and when cells exit the proliferative cell cycle to become quiescent or senescent [20,21].

Positions of chromosome territories can be delineated using *in situ* hybridization (FISH) techniques employing whole chromosome probes [22–24]. Although, three-dimensional FISH assures accurate localization measurements, this technique is time consuming [23,25]. It is thus very difficult to use this technique while looking at global alterations in spatial locations of large number of chromosomes. An easier alternative to this is to perform FISH on completely flattened nuclei (2D-FISH) [2,5]. The ease of this technique and higher probe penetration of flattened nuclei assists in performing large number of hybridizations at once. In addition image capturing is easier in case of 2D-FISH, thus allowing larger numbers of nuclei to be captured. However, one of the major hurdles in performing 2D-FISH is the lack of open access software that could be used to quantify the localization of chromosomal territories.

Previously, a free open-source image analysis tool (IMAJIN COLOC) was developed to do multiple Z plane images (Z stacks) [26]. Another co-localization method has proven to be robust in recognizing co-localizations in the presence of background noise [27]. Several commercial packages for doing Z stack analysis are

also available - Imaris (http://www.bitplane.com/go/products/imaris) and the Zeiss LSM software (http://microscopy.zeiss.com/microscopy/en_de/home.html). However, these are not suited for 2D-analysis. One such application from IPLab Spectrum software (http://www.spectraservices.com/IPLAB.html) that has been used for similar 2D-analyses [2,5,21], has now discontinued the development of the product. Further, an open source package provides a user with the opportunity to fine tune the package according to their requirements.

In the current work, we present software that computes localization of whole chromosomes - Image Analysis of Chromosomes for computing localization (IMACULAT). We partition the cell into concentric elliptical compartments of equal areas, and the variance in the quantity of any chromosome is used to determine its movement in the cell. The results are outputted to a text file, and a corresponding gif image showing the elliptical shells is generated for visual comparison with the original image. Automation allows high throughput analysis for deriving statistics that are used to validate a hypothesis regarding the position of any chromosome. The ImageMagick Perl API libraries (http://www.imagemagick.org/) have been used for pre-processing the images.

In order to validate the functionality of IMACULAT, we have mapped the positions of all human chromosomes in normal human dermal fibroblasts. The locations of these human chromosomes corroborated earlier published studies [2,5,21]. Additionally, in concurrence with previous reports, we observed a gene density based organization of chromosomes with gene-rich chromosomes (19, 17, etc.) occupying the center of the nucleus while gene-poor chromosomes (18, 2, etc.) localizing at the nuclear periphery. Thus, this validation establishes IMACULAT as an automated quantitative methodology that can be routinely used to map positions of components within the nucleus.

Results and Discussion

Understanding the genome and its function is vital in the field of biomedical research. The human genome sequencing project has laid the foundation towards this goal whereby the sequence of 3 billion bases of human DNA was determined and approximately 30,000–40,000 protein coding genes in the human genome have been identified [28,29]. However, it is important to remember that genomes are not a single dimensional entity and elucidation of DNA sequence was only the starting point of genomics research. In reality, it is vital to extrapolate the DNA sequence information from the human genome project onto genome function, which is the major goal of the post-genomic era.

Chromosomes throughout most of the cell's life span occupy a distinct three-dimensional location within the interphase nuclei, which are known as chromosome territories [5,21]. Since cells spend most of their life span in interphase and also most biological activities occur during this phase of the cell cycle, it is important to understand the dynamics of the interphase genome [30]. Spatial organization of chromosomes is thought to affect various important biological processes such as transcription, replication as well as cellular differentiation [8,15,31–35].

Proliferating normal human dermal fibroblasts (NHDFs) were subjected to a standard two-dimensional fluorescence *in situ* hybridization (FISH) to delineate territories for all human chromosomes (22 autosomes, X and Y). A non-random distribution was observed for all human chromosomes in interphase nuclei, and with each chromosome occupying a specific location [2,5,21]. For instance, territories of chromosome 19 are enriched at the center of the nuclei while those of chromosome 12 are known to localize at the nuclear periphery [5,21]. On the other hand, chromosome 8 has an intermediate position within interphase nuclei [5,21]. These spatial distributions of chromosomes within the nuclei have been known to affect genome functions [8,36–38].

Using IMACULAT, we positioned the territories of all human chromosomes within interphase nuclei of normal proliferating human dermal fibroblasts. Representative images and the output of IMACULAT as histograms for each chromosome have been displayed in Fig 1 and 2 respectively. Each nucleus was divided into 5 concentric shells of equal area and the amount of probe corresponding to the chromosome signal, in each shell was quantified (See methods). We observed that % probe signal for most gene-rich chromosomes, for example chromosomes 17 and 19 (Fig 2 panels Q and S, respectively) were enriched in the interior-most shell (Shell 5) and subsequently lowered with decreasing shell number. Thus, the positive slope on the histogram corroborates the interior localization of these chromosome territories (Fig 2 panels Q and S). Similarly, for gene-poor chromosomes, such as chromosomes 13 and 18, the innermost shell (Shell 5) showed the least % probe signal, which increased with radial distance, the signal being the maximum in the outermost shell (Shell 1) (Fig 2 panels M and R, respectively). Hence, the negative slope indicated the already known peripheral location of chromosomes 13 and 18 territories (Fig 2 panels Q and S, respectively). Finally, bell shaped curves of chromosomes, such as chromosome 8, was indicative of its intermediate location within an interphase nucleus (Fig 2 panel H). IMACULAT output for three chromosomes can be accessed at http://www.sanchak.com/imaculat/sampleruns/.

Using IMACULAT, we have corroborated an already existing correlation between gene-density and non-randomness of chromosomal location within an interphase nucleus. For example, the gene-dense chromosome 19 is known to localize at the nuclear interior while nuclear periphery is enriched with gene-poor chromosomes such as chromosome 18 [5,21]. Studies have indicated a relationship between chromosome location and genome function, whereby transcription is enriched at the nuclear center as compared to the periphery [15,31–35]. In corroboration with this, euchromatin is enriched at the nuclear interior while most heterochromatin is localized at a peripheral location within the nucleus [8,39–42]. Spatial distribution within the nucleus is also known to affect other genome functions such as DNA repair [43–47] and replication [48–51]. While a 3D approach to the positioning of chromosomes is increasingly gaining precedence it has been noted that the`2D approach is still the most commonly used and will likely remain the most relevant for a considerably long time' [52]. In the current work, IMACULAT recapitulated that all human chromosome territories occupy a non-random location within the interphase nuclei of human fibroblasts, and thus provides an invaluable computational tool to quantify such spatial distributions.

Materials and Methods

The input to IMACULAT is a rectangular image of an elliptical nucleus which is separated into the background, the cytoplasm and the labeled chromosome(s), each of which has a parameterized color (white, blue and red respectively in the examples presented here) (Fig. 3a). The ImageMagick package parses this image into a grid of pixels (each pixel is represented by the triplet RGB values) of height`H' and width`W' (W = 401, H = 385 for Fig. 3).

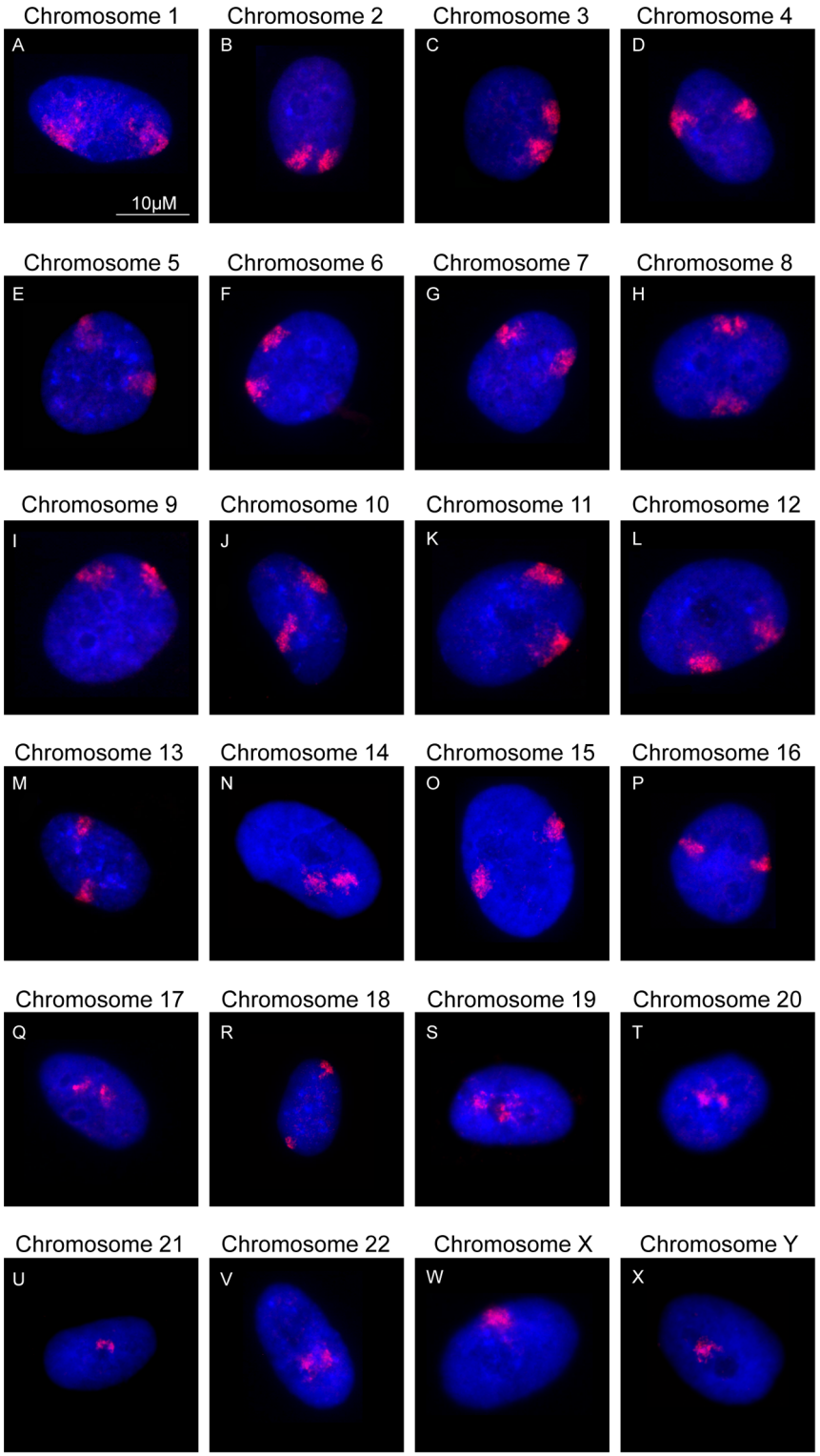

Figure 1. Positions of all chromosomes in normal proliferating human dermal fibroblasts: Images displaying the spatial arrangement of each of the human chromosome territories (in red) in interphase nuclei (stained in blue) of fibroblasts. The numbers on the top of each nucleus indicates the chromosome to which a specific probe was hybridized to, as revealed by FISH. Scale bar = 10 μM.
doi:10.1371/journal.pone.0061386.g001

3.1 Identifying the contour of the nucleus

The first step is to identify the contour of the nucleus. The underlying idea is to scan from the right (or left) from the point x = 1 (x = W for scanning from the left), till we encounter the first nuclear pixel (blue) or chromosome (red), for every height y = 1 to y = H. The contour is thus defined by two columns of height`H' - LCountour and

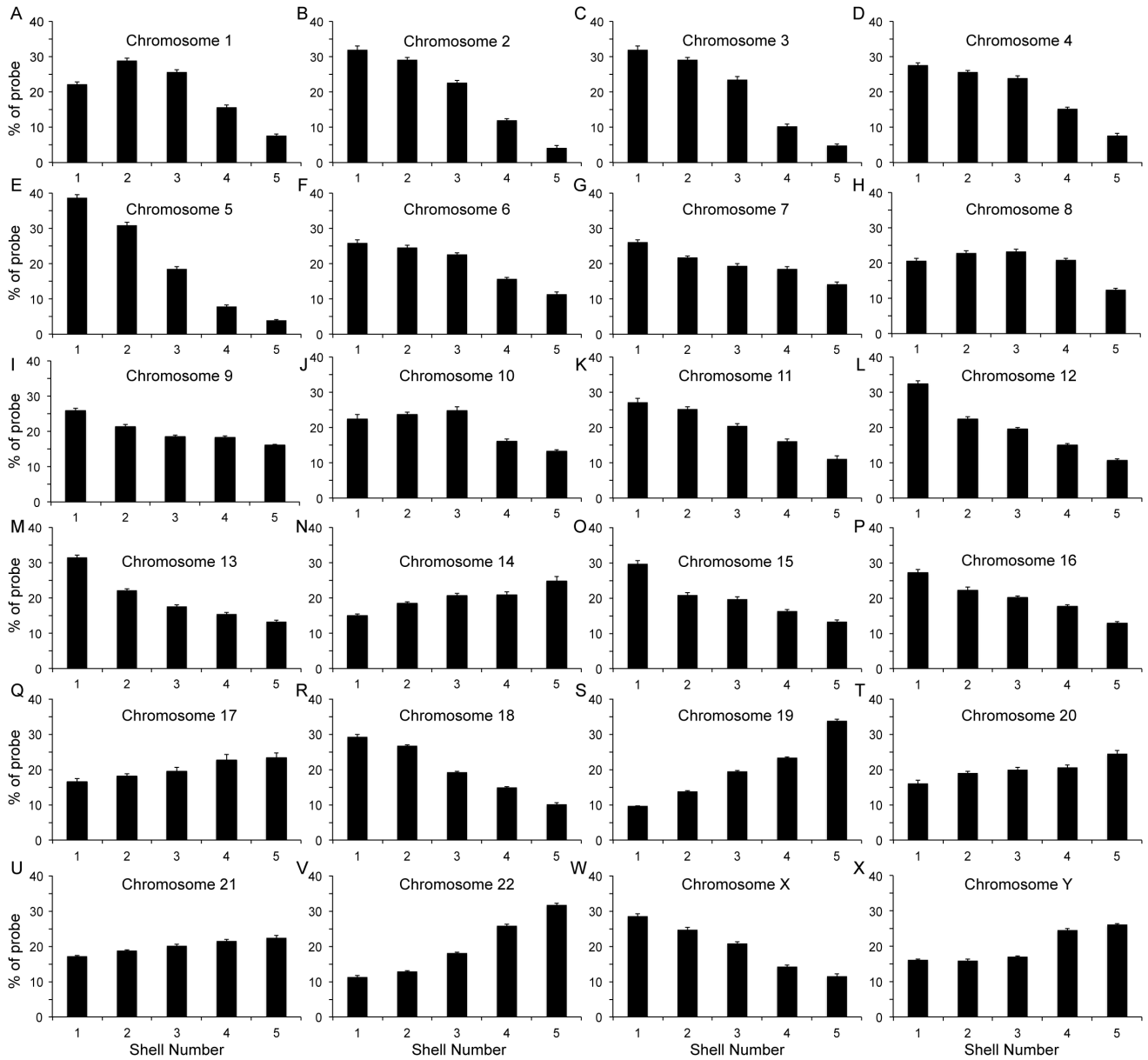

Figure 2. Histograms plotted from output of IMACULAT displaying positions of all human chromosomes in normal proliferating human dermal fibroblasts: Normal human dermal fibroblasts were subjected to standard 2D-FISH assay. At least 100 digital images were analyzed per chromosome by IMACULAT. The graphs display the % probe intensity of each human chromo-some in each of the shells (y-axis), and the shell number on the x-axis. The standard error bars representing the standard errors of mean (SEM) were plotted for each shell for each graph.
doi:10.1371/journal.pone.0061386.g002

RCountour - such that either LCountour[i] = RCountour[i] = 0 (there is no part of the nucleus in this horizontal line), or LCountour[i] < = RCountour[i]. The contour is colored yellow in Fig. 3b.

3.2 Determining the major and minor axes

One cannot make any assumption of the orientation of the nucleus. First, we determine the bounding box coordinates of the nucleus from the contour–$top_{x,y}$, $bottom_{x,y}$, $right_{x,y}$, $left_{x,y}$. The mid point of the nucleus (MPT) is computed as:

$$MPT_x = (right_x + left_x)/2;\ MPT_y = (top_y + bottom_y)/2;$$

The intersection of the major axis to the perimeter is computed as the point (from all the contour points), which has the maximum distance from MPT. Let us denote it as MAJPT1. The line connecting MAJPT1 and MPT is extended till it hits the opposite side of the perimeter, and defines the other end of the major axis (MAJPT2). Since the nucleus is rarely a perfect ellipse, we recalculate the midpoint MPT as:

$$MPT_x = (MAJPT1_x + MAJPT2_x)/2;$$
$$MPT_y = (MAJPT1_y + MAJPT2_y)$$

The minor axis is computed by extending a line perpendicular from MPT, such that it makes two intersections with the perimeter

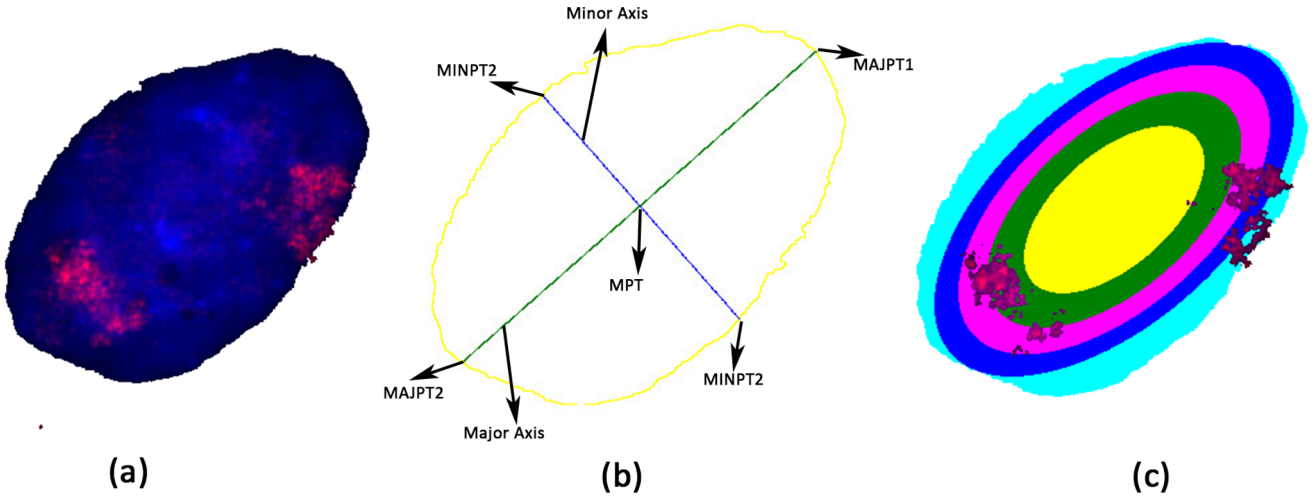

Figure 3. Steps in quantifying chromosome localization: (a) The original image obtained from two-dimensional fluorescence in situ hybridization (FISH). The background, cytoplasm and chromosome are colored white, blue and red respectively. (b) The contour is colored yellow, while the major and minor axes are in green and blue respectively. (c) The nucleus is partitioned into five concentric shells of equal area, and the percentages of chromosome in each shell are computed using the number of red pixels (Table 1).
doi:10.1371/journal.pone.0061386.g003

(MINPT1 and MINPT2). The major and minor axes are shown in Fig. 3b in green and blue respectively.

3.3 Partitioning the nucleus into concentric shells

Let us denote the length of the major and the minor axis as`2A' and `2B' respectively. The area of the ellipse is defined as - AREA = π*A*B. We now proceed to divide the nucleus into N concentric ellipses (five in this case, Fig. 3c). The innermost ellipse should have an area of AREA*1/N, the next ellipse should have area of AREA*2/N and so on. This results in the innermost shell (colored yellow in Fig. 3c) having an area of AREA*1/N, the next shell (colored green in Fig. 3c) with an area of (AREA*2/N–AREA*1/N = AREA*1 = 1/N) and so on. The last shell (colored aqua in Fig. 3c) has by the preceding logic an area of AREA*1/N), although this shell has an irregular shape. Such a bottom-up approach in identifying the shell obviates erosion analysis to smoothen the nuclear periphery. In fact, our analysis is truer in the sense that erosion analysis makes modifications to increase depressed regions and suppress protrusions, although on an average they are expected to offset each other. Another constraint is that for each of the concentric ellipses, the ratio between the major and minor axis (A = B) is to be maintained.

Table 1 shows the number of pixels within each shell, and the distribution of cytoplasm, chromosome and unidentified colors. The colors are identified within a range of values for RGB. For example,`pure' red has the value [1, 0, 0], but a value of [0.9, 0.1, 0.1] is also considered as being red. It can be seen that the unidentified colors are negligible.

3.4 Removing smudges outside the nucleus

Occasionally, we encounter images in which there are smudges outside the nucleus boundary (Fig. 4a). These colored portions pose a problem to the algorithm, which determines the contour, and the major/minor axes of the nucleus (Fig. 4b), and consequently the nucleus partitioning (Fig. 4c). We introduce a pre-processing step to remove these smudges, which results in a representation of the nucleus that corrects the erroneous calculations (Figs. 4 d, e and f). The underlying concept in identifying a color outside the nucleus is to determine the circumference of a specified radius (five pixels in the current examples), and ensure that the circumference has the background color (white in this case). There are two possible cases that will escape this identification algorithm. The first is when the smudge is very close to the nucleus (within the specified radius), and thus should not introduce any significant error if left undetected. The second case occurs when the smudge is larger than the specified radius. Such images are rare, and are removed by visual inspection.

Table 1. Partitioning of the nucleus into concentric ellipses: The areas are computed by the number of pixels as shown in Fig. 2c.

Shell Number	Color	Blue	Red	Others	All	% Blue	% Red	% Others
1	Yellow	12207	10	0	12217	99.9	0.1	0
2	Green	10936	1192	0	12128	90.2	9.8	0
3	Magenta	11015	1221	0	12236	90	10	0
4	Blue	11483	716	5	12204	94.1	5.9	0
5	Aqua	11406	653	34	12093	94.3	5	0.3

The cytoplasm and labeled chromosome are colored blue and red respectively. Any color not recognized as either of these two colors is specified as`Others'. Shells are numbered from the periphery inwards.
doi:10.1371/journal.pone.0061386.t001

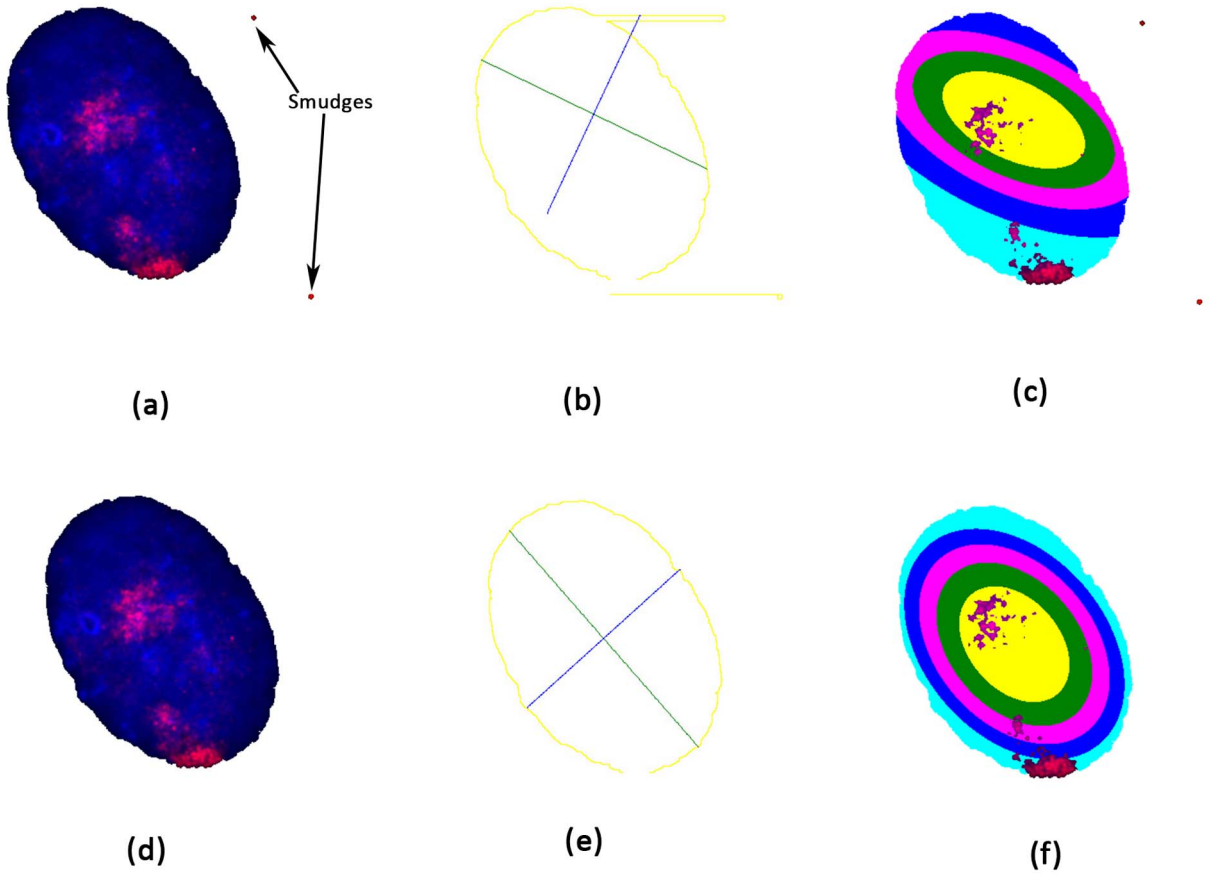

Figure 4. Steps in removing smudges outside the nucleus boundary: (a) There are a couple of unwanted smudges outside the nucleus boundary colored red. (b) These smudges pose a problem while computing the contour, which assumes the presence of any color other than background color (white) as the beginning of the nucleus. The major and minor axes can be seen to be erroneous. (c) Consequently, the partitioning of the nucleus is incorrect too. (d) The pre-processing step removes the smudges. See Methods section for the detailed algorithm. (e) The computation of the contour, the major and the minor axis are now correct. (f) The erroneous partitioning is thus fixed.
doi:10.1371/journal.pone.0061386.g004

3.5 Installation, running the program and analyzing the results

The IMACULAT package is written in Perl on Ubuntu. Hardware requirements are modest - all results presented here are from a simple workstation (8GB ram) and runtimes per image were a few Minutes, at the most. The source code and manual are made available at www.sanchak.com/imaculat.html. The installation requires the following supplementary packages - ImageMagick (available at http://www.imagemagick.org/) and the Perl api package (Image::Magick), which can be obtained from www.cpan.org.

In order to simplify running the program, we have created a wrapper C-shell script that takes two parameters - a file containing the name of the image files to be processed, and the name of the results directory. The output is an Excel (.xls) sheet, which details the % of the probe present in each shell. Other outputs show the identified colors in the images as intermediate files. We have provided three sample directories, which contain the original images and the IMACULAT results, at www.sanchak.com/imaculat/sampleruns.tgz. They are also present in a directory structure for easy browsing at www.sanchak.com/imaculat/sampleruns/.

3.6 In *vitro* methods

Proliferating normal human dermal fibroblasts (NHDFs) [Lonza] were maintained in 15% FBS-DMEM. Spatial locations of chromosomes were delineated using standard two-dimensional fluorescence *in situ* hybridization protocol [2]. Briefly, cells were trypsinized, treated with hypotonic solution and fixed with methanol:acetic acid (3:1). Further, cells were taken through an ethanol row followed by denaturation using 70% (v/v) formamide at 70 °C and hybridization with whole chromosome probes [Applied Spectral Imaging]. The slides were then washed and mounted in Vectashield mounting media containing DAPI [Vectashield]. At least 100 images were captured per chromosome using Zeiss Axiovert 200 microscope (Axiovision software). Spatial positions of chromosome territories in these images were obtained by running them through IMACULAT. Histograms displaying these results and standard error bars representing the +/− standard error of mean (SEM) were plotted.

Acknowledgments

We are grateful to Bjarni Asgeirsson from the Science Institute, Department of Biochemistry, University of Iceland and Mugdha Kulashreshtha, Department of Biological Sciences, Tata Institute of Fundamental Research, India for help in correcting the revised manuscript.

Author Contributions

Conceived and designed the experiments: IM SC. Performed the experiments: IM SC. Analyzed the data: IM SC. Contributed reagents/materials/analysis tools: IM SC. Wrote the paper: IM SC BJR.

References

1. Alberts B, Johnson A, Lewis J, Ra M, Roberts K, et al. (2002) Molecular Biology of the Cell. Garland Science Taylor & Francis Group, 4th edition, City.
2. Croft JA, Bridger JM, Boyle S, Perry P, Teague P, et al. (1999) Differences in the localization and morphology of chromosomes in the human nucleus. J Cell Biol 145: 1119–1131.
3. Cremer C, Zorn C, Cremer T (1974) An ultraviolet laser microbeam for 257 nm. Microsc Acta 75: 331–337.
4. Zorn C, Cremer C, Cremer T, Zimmer J (1979) Unscheduled DNA synthesis after partial UV irradiation of the cell nucleus. Distribution in interphase and metaphase. Exp Cell Res 124: 111–119.
5. Boyle S, Gilchrist S, Bridger JM, Mahy NL, Ellis JA, et al. (2001) The spatial organization of human chromosomes within the nuclei of normal and emerin-mutant cells. Hum Mol Genet 10: 211–219.
6. van Driel R, Humbel B, de Jong L (1991) The nucleus: a black box being opened. J Cell Biochem 47: 311–316.
7. Strouboulis J, Wolffe AP (1996) Functional compartmentalization of the nucleus. J Cell Sci 109 (Pt 8): 1991–2000.
8. Foster HA, Bridger JM (2005) The genome and the nucleus: a marriage made by evolution. Genome organisation and nuclear architecture. Chromosoma 114: 212–229.
9. Bridger JM, Foeger N, Kill IR, Herrmann H (2007) The nuclear lamina. Both a structural framework and a platform for genome organization. FEBS J 274: 1354–1361.
10. Parada L, Misteli T (2002) Chromosome positioning in the interphase nucleus. Trends Cell Biol 12: 425–432.
11. Meaburn KJ, Misteli T, Soutoglou E (2007) Spatial genome organization in the formation of chromosomal translocations. Semin Cancer Biol 17: 80–90.
12. Bridger JM, Bickmore WA (1998) Putting the genome on the map. Trends Genet 14: 403–409.
13. Cremer T, Cremer C (2001) Chromosome territories, nuclear architecture and gene regulation in mammalian cells. Nat Rev Genet 2: 292–301.
14. Gasser SM (2002) Visualizing chromatin dynamics in interphase nuclei. Science 296: 1412–1416.
15. Kim SH, McQueen PG, Lichtman MK, Shevach EM, Parada LA, et al. (2004) Spatial genome organization during T-cell di erentiation. Cytogenet Genome Res 105: 292–301.
16. Kuroda M, Tanabe H, Yoshida K, Oikawa K, Saito A, et al. (2004) Alteration of chromosome positioning during adipocyte di erentiation. J Cell Sci 117: 5897–5903.
17. Parada LA, McQueen PG, Misteli T (2004) Tissue-specific spatial organization of genomes. Genome Biol 5: R44.
18. Panning MM, Gilbert DM (2005) Spatio-temporal organization of DNA replication in murine embryonic stem, primary, and immortalized cells. J Cell Biochem 95: 74–82.
19. Casolari JM, Brown CR, Drubin DA, Rando OJ, Silver PA (2005) Developmentally induced changes in transcriptional program alter spatial organization across chromosomes. Genes Dev 19: 1188–1198.
20. Bridger JM, Boyle S, Kill IR, Bickmore WA (2000) Re-modelling of nuclear architecture in quiescent and senescent human fibroblasts. Curr Biol 10: 149–152.
21. Mehta IS, Amira M, Harvey AJ, Bridger JM (2010) Rapid chromosome territory relocation by nuclear motor activity in response to serum removal in primary human fibroblasts. Genome Biol 11: R5.
22. Cremer T, Lichter P, Borden J, Ward DC, Manuelidis L (1988) Detection of chromosome aberrations in metaphase and interphase tumor cells by in situ hybridization using chromosome-specific library probes. Hum Genet 80: 235–246.
23. Lichter P, Cremer T, Borden J, Manuelidis L, Ward DC (1988) Delineation of individual human chromosomes in metaphase and interphase cells by in situ suppression hybridization using recombinant DNA libraries. Hum Genet 80: 224–234.
24. Manuelidis L (1985) Indications of centromere movement during interphase and differentiation. Ann N Y Acad Sci 450: 205–221.
25. Solovei I, Cavallo A, Schermelleh L, Jaunin F, Scasselati C, et al. (2002) Spatial preservation of nuclear chromatin architecture during three-dimensional fluorescence in situ hybridization (3D-FISH). Exp Cell Res 276: 10–23.
26. Goucher DR, Wincovitch SM, Gar eld SH, Carbone KM, Malik TH (2005) A quantitative determination of multi-protein interactions by the analysis of confocal images using a pixel-by-pixel assessment algorithm. Bioinformatics 21: 3248–3254.
27. Wang Y, Ledgerwood C, Grills C, Fitzgerald DC, Hamilton PW (2012) A robust co-localisation measurement utilising z-stack image intensity similarities for biological studies. PLoS ONE 7: e30632.
28. Lander ES, Linton LM, Birren B, Nusbaum C, Zody MC, et al. (2001) Initial sequencing and analysis of the human genome. Nature 409: 860–921.
29. Venter JC, Adams MD, Myers EW, Li PW, Mural RJ, et al. (2001) The sequence of the human genome. Science 291: 1304–1351.
30. Cooper GM (2000) The Cell - A Molecular Approach 2nd Edition. Sunderland (MA): Sinauer Associates.
31. Brown KE, Baxter J, Graf D, Merkenschlager M, Fisher AG (1999) Dynamic repositioning of genes in the nucleus of lymphocytes preparing for cell division. Mol Cell 3: 207–217.
32. Delaire S, Huang YH, Chan SW, Robey EA (2004) Dynamic repositioning of CD4 and CD8 genes during T cell development. J Exp Med 200: 1427–1435.
33. Hewitt SL, High FA, Reiner SL, Fisher AG, Merkenschlager M (2004) Nuclear repositioning marks the selective exclusion of lineage-inappropriate transcription factor loci during T helper cell di erentiation. Eur J Immunol 34: 3604–3613.
34. Zink D, Amaral MD, Englmann A, Lang S, Clarke LA, et al. (2004) Transcription-dependent spatial arrangements of CFTR and adjacent genes in human cell nuclei. J Cell Biol 166: 815–825.
35. Szczerbal I, Foster HA, Bridger JM (2009) The spatial repositioning of adipogenesis genes is correlated with their expression status in a porcine mesenchymal stem cell adipogenesis model system. Chromosoma 118: 647–663.
36. Branco MR, Pombo A (2006) Intermingling of chromosome territories in interphase suggests role in translocations and transcription-dependent associations. PLoS Biol 4: e138.
37. Fraser P, Bickmore W (2007) Nuclear organization of the genome and the potential for gene regulation. Nature 447: 413–417.
38. Meaburn KJ, Misteli T (2007) Cell biology: chromosome territories. Nature 445: 379–781.
39. Andrulis ED, Neiman AM, Zappulla DC, Sternglanz R (1998) Perinuclear localization of chromatin facilitates transcriptional silencing. Nature 394: 592–595.
40. Brown KE, Guest SS, Smale ST, Hahm K, Merkenschlager M, et al. (1997) Association of transcriptionally silent genes with Ikaros complexes at centromeric heterochromatin. Cell 91: 845–854.
41. Cockell M, Gasser SM (1999) Nuclear compartments and gene regulation. Curr Opin Genet Dev 9: 199–205.
42. Ferreira J, Paolella G, Ramos C, Lamond AI (1997) Spatial organization of large-scale chromatin domains in the nucleus: a magni ed view of single chromosome territories. J Cell Biol 139: 1597–1610.
43. Falk M, Lukasova E, Kozubek S (2008) Chromatin structure influences the sensitivity of DNA to gamma-radiation. Biochim Biophys Acta 1783: 2398–2414.
44. Folle GA (2008) Nuclear architecture, chromosome domains and genetic damage. Mutat Res 658: 172–183.
45. Gazave E, Gautier P, Gilchrist S, Bickmore WA (2005) Does radial nuclear organisation influence DNA damage? Chromosome Res 13: 377–388.
46. Martinez-Lopez W, Folle GA, Obe G, Jeppesen P (2001) Chromosome regions enriched in hyperacetylated histone H4 are preferred sites for endonuclease- and radiation-induced breakpoints. Chromosome Res 9: 69–75.
47. Sanders MH, Bates SE, Wilbur BS, Holmquist GP (2004) Repair rates of R-band, G-band and C-band DNA in murine and human cultured cells. Cytogenet Genome Res 104: 35–45.
48. Federico C, Cantarella CD, Di Mare P, Tosi S, Saccone S (2008) The radial arrangement of the human chromosome 7 in the lymphocyte cell nucleus is associated with chromosomal band gene density. Chromosoma 117: 399–410.
49. Gilbert N, Gilchrist S, Bickmore WA (2005) Chromatin organization in the mammalian nucleus. Int Rev Cytol 242: 283–336.
50. Grasser F, Neusser M, Fiegler H, Thormeyer T, Cremer M, et al. (2008) Replication-timing-correlated spatial chromatin arrangements in cancer and in primate interphase nuclei. J Cell Sci 121: 1876–1886.
51. Nogami M, Nogami O, Kagotani K, Okumura M, Taguchi H, et al. (2000) Intranuclear arrangement of human chromosome 12 correlates to large-scale replication domains. Chromosoma 108: 514–522.
52. Zinchuk V, Grossenbacher-Zinchuk O (2009) Recent advances in quantitative colocalization analysis: focus on neuroscience. Prog Histochem Cytochem 44: 125–172.